

# MOVING-MAGNET PLANAR ACTUATOR WITH INTEGRATED ACTIVE MAGNETIC BEARING

J.W. Jansen, C.M.M. van Lierop, E.A. Lomonova, A.J.A. Vandenput  
Department of Electrical Engineering, Eindhoven University of Technology  
Eindhoven, The Netherlands

## INTRODUCTION

In recent years, magnetically levitated planar actuators have been developed for demanding applications such as wafer stages. Although the translator of these actuators can move over relatively large distances in the  $xy$ -plane only, it has to be controlled in six degrees-of-freedom (DOF) because of the active magnetic bearing. These actuators have either moving magnets and stationary coils [1] [2] or moving coils and stationary magnets [3]. The coils in the actuator are simultaneously used for the propulsion in the  $xy$ -plane as well as for the 4-DOF active magnetic bearing.

The advantage of a moving-magnet topology is that the coils and, therefore, the power supply and the cooling are located at the stationary part of the actuator. Consequently, no cable to the moving part is necessary. However, only the coils below the magnet array significantly contribute to the propulsion and the active magnetic bearing. For this reason, the set of active coils changes with the position of the translator in a long-stroke moving-magnet planar actuator.

Contrary to moving-coil planar actuators, symmetries in the design of a long-stroke moving-magnet actuator cannot be used to decouple the force and the torque. The strong coupling between the degrees-of-freedom combined with the need to switch between coil-sets requires new commutation techniques [4] and, therefore, new design methods.

In this paper a long-stroke moving-magnet planar actuator with integrated magnetic bearing is presented. The position dependent condition number of the commutation and decoupling matrix is used as a design criterion to predict the 6-DOF controllability of the topology.

## TOPOLOGY

The topology of the planar actuator is shown in Figs. 1 and 2. The dimensions and properties are summarized in Table 1. The translator consists of a Halbach permanent-magnet array

which is glued to an aluminum carrier. A Halbach permanent-magnet array is used as it increases the magnetic flux density near the coils. Although the extra permanent magnets, which are magnetized in the  $x$ - and  $y$ -directions, increase the mass of the translator, the power dissipation of the actuator is smaller compared to an actuator without these extra magnets.

The stator consists of 84 coils in a herringbone pattern. At most 24 adjacent coils are used simultaneously to control the translator in six degrees-of-freedom. All coils are connected to single-phase power amplifiers.

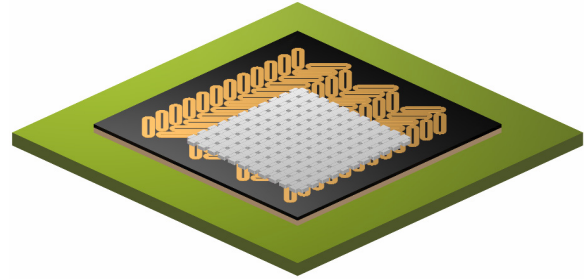


FIGURE 1. Overview of the six degree-of-freedom moving-magnet planar actuator.

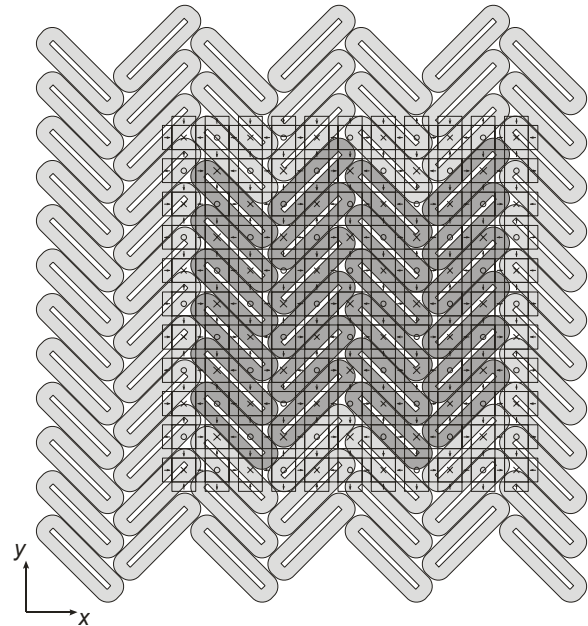


FIGURE 2. Moving-magnet planar actuator (top view).

The coils are rotated 45 degrees with respect to the magnet array. In this way, the coils can be made rectangular instead of square which will decrease the power dissipation of the actuator.

Fig. 3 shows a detail of the actuator. In the figure two groups of three coils are shown. Although the coils are individually excited by single-phase power amplifiers, the coils in each group are positioned according to a three-phase system to reduce the influence of higher harmonics of the magnetic flux density distribution of the translator on the force and the torque. Each group can produce force in two directions independent of the position of the magnet array. Both groups can produce levitation force (z-direction). The force produced in the  $xy$ -plane  $F_{xy}$  by both groups is orthogonal as indicated by the arrows in Fig. 3. Because the length  $l$  of the coils is equal to  $2n\tau_n$ , where  $n$  is an integer (for these coils  $n=2$ ) and  $\tau_n$  is the pole pitch as defined in Fig. 3, the force production in the  $xy$ -plane is physically decoupled [3] [5]. This reduces cross-talk between the degrees-of-freedom and, therefore, simplifies the modeling of the force and the torque in the actuator.

TABLE 1. Properties and dimensions of the actuator.

Size translator	300x300 mm
Mass translator	8 kg
Mechanical clearance (z-dir.)	1 – 2 mm
Stroke (xy-plane)	230x230 mm
Max speed (xy-plane)	1 m/s
Max acceleration (xy-plane)	10 m/s <sup>2</sup>
Cooling medium	Water

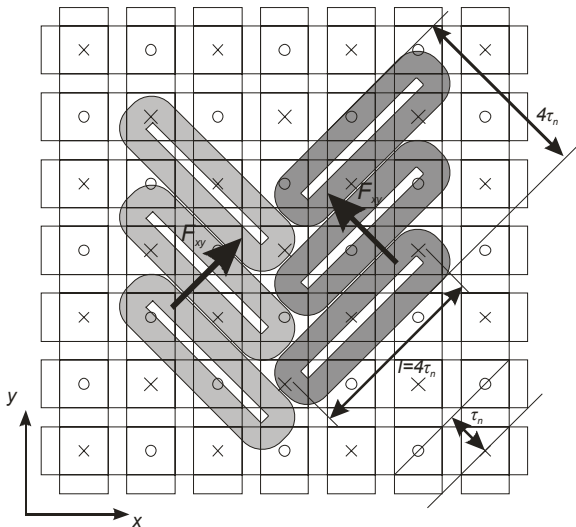


FIGURE 3. Detail of the actuator with two 3-phase coil groups.

## COMMUTATION AND SWITCHING

Because the coils are responsible for both the propulsion of the magnet array and its active magnetic bearing, both the torque and the force produced by these coils should be controlled accurately. Fig. 4 shows the controller and the actuator schematically. The actuator is modeled by a position dependent non-linear mapping  $\Gamma$ , which maps the active currents  $\vec{i}$  on the force and torque vector  $\vec{w}$ , and by linear time invariant (LTI) plant dynamics. In this approach rigid body dynamics are assumed.

The LTI controller calculates a force and torque set-point, the desired wrench  $\vec{w}^*$ , which should be converted to current set-points  $\vec{i}^*$  for the active coils in the actuator. DQ0-decomposition cannot be used as a commutation algorithm as it can only decouple the force and not the torque in this actuator. Because the 6-DOF actuator is clearly over-actuated, there is a set of transformations which provide a proper linearization and decoupling of the degrees-of-freedom [4]. A solution to this problem is to minimize the ohmic losses in the coils, i.e.

$$\min_{\Gamma(\vec{p})\vec{i}=\vec{w}^*} \|\vec{i}^*\| = \|\Gamma^{-1}(\vec{p})\vec{w}^*\|, \quad (1)$$

where  $\Gamma(\vec{p})$ , is a matrix which contains the mapping of the current in the active coils on the force and torque exerted on the translator as a function of the position and the orientation of the translator in six degrees-of-freedom  $\vec{p}$ . The minimization in (1) can be solved by calculating the Moore-Penrose inverse of  $\Gamma(\vec{p})$ .

To decrease the computation time of the commutation algorithm, the transfer functions in  $\Gamma(\vec{p})$  are analytical equations which assume an infinitely long magnet array and which can be evaluated fast [5]. Because the end-effects of the magnet array are not included in these equations, the model deviates for the coils which are near the edge of the magnet array.

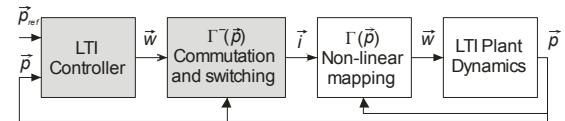


FIGURE 4. Simplified model of the actuator and controller (controller and commutation in gray), assuming ideal power amplifiers ( $\vec{i} = \vec{i}^*$ ).

Therefore, these coils are actively switched off by smooth weighing functions  $\Delta(\rho_x, \rho_y)$ , which depend on the position of the translator in the  $xy$ -plane,  $\rho_x$  and  $\rho_y$ .

The force and torque can be decoupled again by minimizing the ohmic losses in the coils [4]:

$$\min_{\Gamma(\bar{\rho})\bar{i}^*=\bar{w}^*} \|\bar{i}^*\|_{\Delta^{-1}(\rho_x, \rho_y)} = \|\Gamma^{-}(\bar{\rho})\bar{w}^*\|, \quad (2)$$

where:

$$\Gamma^{-}(\bar{\rho}) = \Delta(\rho_x, \rho_y)\Gamma^{\top}(\bar{\rho})(\Gamma(\bar{\rho})\Delta(\rho_x, \rho_y)\Gamma^{\top}(\bar{\rho}))^{-1}. \quad (3)$$

When the translator moves in the  $xy$ -plane, there are 15 to 24 simultaneously active coils. In total there are 28 different sets of active coils. The weighing functions smoothly switch the coils on and off at a transition between two different sets of coils.

The effect of the weighing function is illustrated in Fig. 5. In the bottom-left figure the weighing functions do not penalize any coil and all 24 coils are active. When the translator moves in the  $x$ -direction, the active coils in the left column will be smoothly switched off. After they are switched off, the adjacent coils in the outer right column will be smoothly switched on (not shown). At the transition, only 18 coils are active (bottom-right figure). When the translator moves

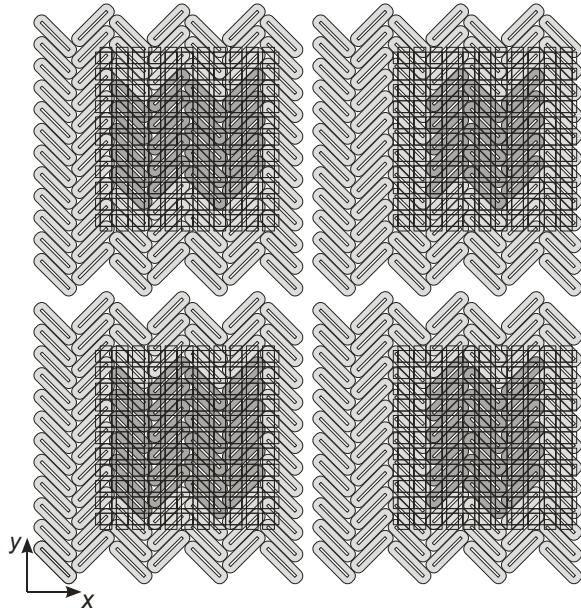


FIGURE 5. Active coils at the transitions between different sets of coils.

in the  $y$ -direction only 20 coils are active at the transition between two different sets of coils (top-left figure). In the worst case situation (top-right figure), 9 coils are penalized by the weighing function and are switched off.

### CONDITION NUMBER

Both the controllability and the power dissipation of a planar actuator topology are influenced by the commutation and switching algorithm. Because evaluating a large number of topologies with an accurate electromagnetic model is very time consuming, the condition number of  $\Gamma^{-}(\bar{\rho})$  is calculated on a grid in the  $xy$ -plane to predict the controllability of a topology. If the condition number of  $\Gamma^{-}(\bar{\rho})$  is sufficiently small, then all force and torque combinations can be achieved. Generally, a low condition number also results in small force and torque ripples.

Fig. 6 shows the condition number of the presented topology over a part of the stroke of the actuator. The switching between different sets of coils in the  $x$ -direction is most clearly visible in the condition number.

Fig. 7 shows the estimated ohmic losses for two load situations, levitation of the translator only and levitation and acceleration in the  $xy$ -plane of the translator. The losses are strongly influenced by the switching between the different coil sets.

Figs. 8 and 9 show the predicted open-loop force and torque ripple for the second load situation. The force and torque ripples are small and no cross-talk between the force and the torque is visible.

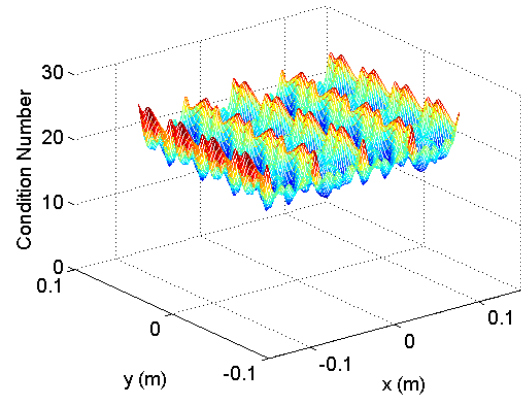


FIGURE 6. The condition number of  $\Gamma^{-}(\bar{\rho})$ .

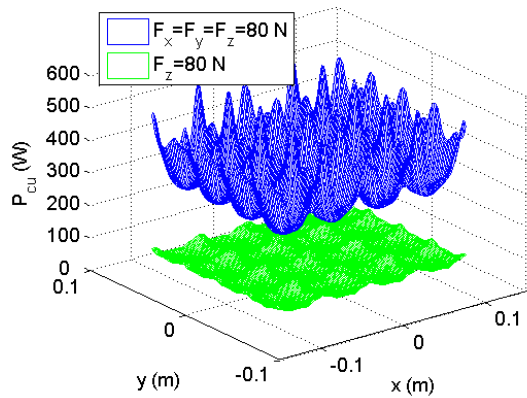


FIGURE 7. Predicted power dissipation (2 mm mechanical clearance between the stator and the translator).

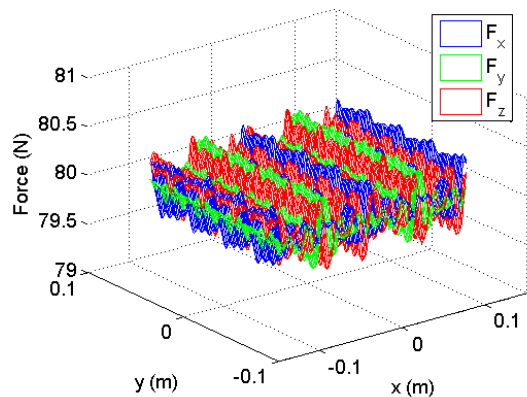


FIGURE 8. Predicted force ( $F_x = F_y = F_z = 80 \text{ N}$  and  $T_x = T_y = T_z = 0 \text{ Nm}$ ).

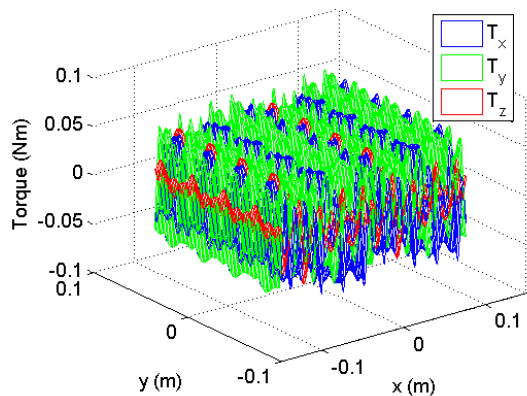


FIGURE 9. Predicted torque ( $F_x = F_y = F_z = 80 \text{ N}$  and  $T_x = T_y = T_z = 0 \text{ Nm}$ ).

## CONCLUSIONS

A moving-magnet planar actuator with integrated magnetic bearing has been presented. Simulations show that the degrees-of-freedom can be sufficiently decoupled and that the force and torque ripples are small. The switching between different sets of coils, necessary to achieve long-stroke motion, significantly influences the power dissipation.

## ACKNOWLEDGEMENT

The authors would like to thank Mr. Marijn Uyt De Willigen for his assistance with the set-up. The authors would also like to thank ASML, Assembléon, Philips Applied Technologies, Prodrive, Tecnotion and Vacuumschmelze for their valuable contributions and support. This IOP-EMVT project is funded by SenterNovem. SenterNovem is an agency of the Dutch Ministry of Economical Affairs.

## REFERENCES

- [1] W. J. Kim, D. L. Trumper, and J. H. Lang, "Modeling and vector control of a planar magnetic levitator," *IEEE Trans. Ind. Applicat.*, vol. 34, no. 6, pp. 1254–1262, Nov/Dec 1998.
- [2] A. J. Hazelton, M. B. Binnard, and J. M. Gery, "Electric motors and positioning devices having moving magnet arrays and six degrees of freedom," U.S. Patent 6,208,045, 27 March 2001.
- [3] J. C. Compter, "Electro-dynamic planar motor," *Precision Engineering*, vol. 28, no. 2, pp. 171–180, Apr 2004.
- [4] C. M. M. van Lierop, J. W. Jansen, A. A. H. Damen, and P. P. J. van den Bosch, "Control of multi-degree-of-freedom planar actuators," in *Proc. of the 2006 IEEE International Conference on Control Applications, CCA 2006*, Munich, Germany, Oct 2006, in press.
- [5] J. W. Jansen, E. A. Lomonova, A. J. A. Vandenput, and C. M. M. van Lierop, "Analytical model of a magnetically levitated linear actuator," in *Conf. Rec. 2005 Industry Applications Conference, 40<sup>th</sup> IAS Annual Meeting*, Oct 2005, pp. 2107–2113.